ARTICLE TYPE

Picosecond self-diffusion in ethanol-water mixtures[†]

Tilo Seydel,[a] **Robert M. Edkins,**[b] **and Katharina Edkins**[*c]

We report the self-diffusion in ethanol-water mixtures as a function of the water-ethanol ratio measured at different temperatures using quasi-elastic neutron spectroscopy (QENS). For our protiated samples, QENS is mainly sensitive to the dominant ensemble-averaged incoherent scattering from the hydrogen atoms of the liquid mixtures. The energy range and resolution render our experiment sensitive to the picosecond time scale and nanometer length scale. These observation scales complement different scales accessible by nuclear magnetic resonance techniques. Subsequent to testing different models, we find that a simple jump-diffusion model averaging over both types of molecules, water and ethanol, best fits our data.

1 Introduction

Aqueous ethanol has gained significant attention in a wide variety of scientific applications. Even though pure water is the most important solvent in nature, these mixtures of water and ethanol in various stoichiometries form the basis of a number of beverages[1,2] and are used in a great number of applications, such as pharmaceutical materials,[3,4] sustainable synthetic routes in green chemistry,[5] and biofuels,[6] to name but a few. Especially in food science and pharmaceutical applications, ethanol is widely used for its antibacterial and preservative activity.[7] In the formulation of medicines, ethanol is deemed non-hazardous and is generally recognised as safe by the FDA. Thus, a plethora of classical formulations as well as novel therapeutic platforms are based on this solvent or use it during the manufacturing process.[4]

On the physicochemical level, water-ethanol mixtures display a non-monotonous dependence of macroscopic properties on the mixing ratio, such as volume and viscosity,[8] and refractive index.[9] Especially the volume contraction and with that the increase in viscosity has attracted great interest,[10,11] with the viscosity attaining a maximum near 0.2 mole fraction ethanol in the ethanol-water mixture at ambient temperature.[8]

Whilst earlier studies have concentrated on the macroscopic properties of the highly hydrogen-bonded solvent mixtures,[12,13] more recent investigations aim to understand the non-ideal behaviour on the molecular level. Ethanol and other lower alcohols have been studied to elucidate their highly hydrogen-bonded structure using various spectroscopic techniques.[14–16] Results from neutron diffraction on water-ethanol mixtures specifically suggest that at low ethanol concentrations the alcohol has little effect on the water hydrogen bond network and that apolar groups of the alcohol located inside water cavities tend to stabilize the water network.[17] This micro-heterogeneity[18] has particular impact on biological applications, as protein folding is highly dependent on hydration, and partitioning of parts of the protein into the hydrophobic clusters may give information about processes in living cells.[19–21]

Most of the mentioned studies focus on a static picture of the alcohol water mixtures, whilst the self- or, synonymously, tracer diffusion paint the dynamic picture. Diffusion of these mixtures has been investigated systematically for methanol/water already some time ago using radioactive tracer techniques.[22] More recently, the self-diffusion coefficients of water and ethanol in water-ethanol mixtures have been simulated[23–25] and experimentally determined using pulse field gradient nuclear magnetic resonance (PFG-NMR) techniques on the millisecond timescale.[26,27] Both the simulations and the NMR results display a minimum in the tracer diffusion of both the water and ethanol constituents near the position of the macroscopic viscosity maximum. Moreover, both constituents have similar self-diffusion coefficients.[25] To probe solvent diffusion coefficients on the picosecond timescale, quasi-elastic neutron spectroscopy (QENS) is used, and has been successfully applied to methanol/water mixtures[15] as well as longer alcohols such as butyl alcohol mixed with water.[28] However, comprehensive neutron data on the picosecond self-diffusion in water-ethanol mixtures as a function of the mixing ratio have been missing. Since we have recently shown that apparent diffusion coefficients determined by NMR and QENS are not directly comparable,[29] it appears timely to investi-

gate these mixtures using neutron spectroscopy and to provide this data for future reference. Incoherent QENS accesses the ensemble-averaged single-particle self-correlation function on the nanometer length scale and picosecond to nanosecond time scale. Here, we systematically explore the prevailing incoherent scattering from protiated water-ethanol mixtures at different mixing ratios and for different temperatures. Such data may also be of value as additional information to compare with molecular dynamics simulations.

2 Experiments and methods

This study is based on the use of mixtures of fully protiated water and ethanol. Whilst partial deuteration would allow for a reasonably easy distinction between the two components of the mixtures, the increased mass of the deuterated molecules will itself influence their diffusion coefficients. We have thus decided to determine fully protiated samples first with future measurements on deuterated samples planned. The water-ethanol samples were prepared by measuring exact volumes of the individual components, which were subsequently mixed in a glass vial sealed by a screw-on cap. Solvent volumes were measured with a 0.25 ml Hamilton syringe at ambient temperature of 294 K, as secured by using a preheated water bath. The two solvent aliquots were thoroughly mixed in a sealed vial and transferred into the sample holders before being sealed for measurement.

QENS experiments have been carried out on the cold neutron chopper spectrometer LET[30] at the pulsed neutron source of the ISIS Neutron and Muon Facility at the Rutherford Appleton Laboratory. The samples were filled in double-walled cylindrical aluminium sample holders with 0.1 mm gap size and sealed against vacuum with indium wire. The samples were held in a closed-cycle cryostat inside the neutron spectrometer during the data acquisition. The temperature was controlled to better than ± 0.01 K using local resistance heating on the sample holders.

The instrument setup allowed us to record data quasi-simultaneously at three different incident energies, namely 0.74, 1.38, and 3.4 meV. The background was measured by recording the scattering signal from an empty sample cell, but found to be negligibly weak compared to the scattering from the sample solutions at 3.4 meV incident energy. The empty cell signal was subtracted from the sample spectra prior to the fitting.

The data reduction was carried out using *python* scripts provided by the LET instrument team as part of the *Mantid* software (www.mantidproject.org).[31] The accessible scattering vector range was binned into equidistant q-slices with width $\Delta q = 0.1$ Å^{-1}. Subsequently, all fits of the QENS spectra were performed using *python 3.5.2* scripts, notably employing the *curve_fit* command from *scipy.optimize*. All plots

were created using *python 3.5.2* and the associated *matplotlib* package.

The spectrometer resolution function $\mathscr{R}(q, \omega)$, depending on the momentum transfer (synonymously: scattering vector) q and energy transfer $\hbar\omega$, was measured using vanadium foil as a sample and a water-ethanol mixture (0.16 mole fraction ethanol) at $T = 150$ K, i.e. in the frozen state, and the function was subsequently modeled by fitting a sum of five Gaussian functions (see figure S1 in the Electronic Supporting Information ESI). The low-temperature sample better mimicked the sample geometry and was therefore used in the further analysis as resolution.

3 Results and Discussion

The reduced spectra were fitted by $\mathscr{R}(q, \omega) \otimes S(q, \omega)$ using the model scattering function $S(q, \omega)$ established for pure water (H_2O)[32], being implemented as
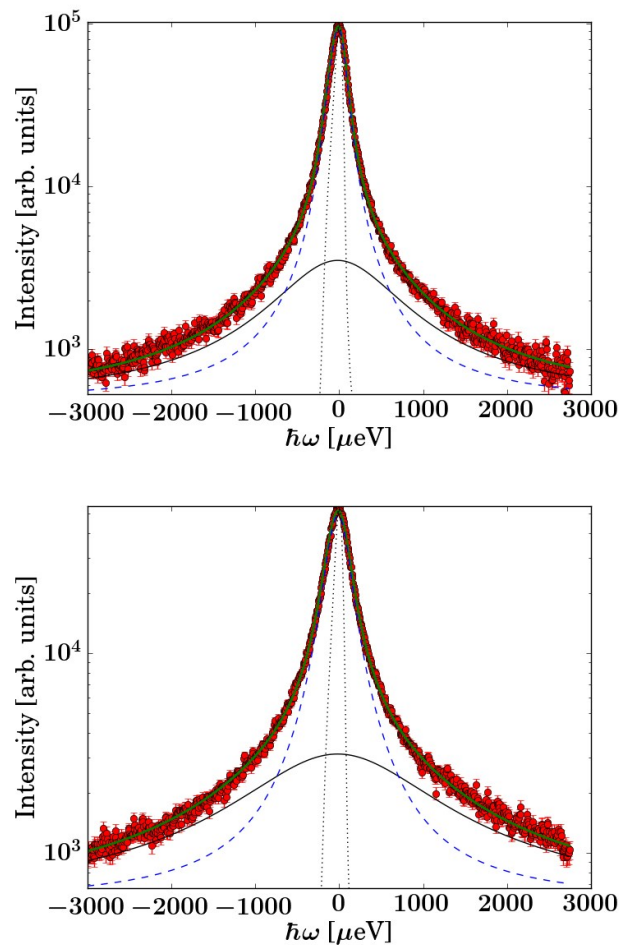
$$S(q, \omega) = \quad a_1(q) \frac{1}{\pi} \frac{\sigma_1(q)}{\sigma_1(q)^2 + \omega^2}$$
$$+ a_2(q) \frac{1}{\pi} \frac{\sigma_2(q)}{\sigma_2(q)^2 + \omega^2} + b(q). \quad (1)$$

Therein, $a_{1,2}(q)$, $\sigma_{1,2}(q)$, and $b(q)$ are scalar parameters. $b(q)$ accounts for a small apparent flat background arising from instrument, sample, and sample environment contributions. Since the model equation 1 contains Lorentzians only and the resolution function can be described by a sum of Gaussians, the convolution $\mathscr{R}(q, \omega) \otimes S(q, \omega)$ was analytically implemented by Voigt functions (calculated employing the real part of the Faddeeva function from *scipy.special*). σ_1 can be associated with the center-of-mass diffusion of both the water and ethanol solvent molecules. $a_{1,2}(q)$, $\sigma_2(q)$, and $b(q)$ were fitted for each q independently (figure S4 in the ESI). In contrast, in a global fit approach of all q at once, the jump-diffusion process implemented by the relation[33]
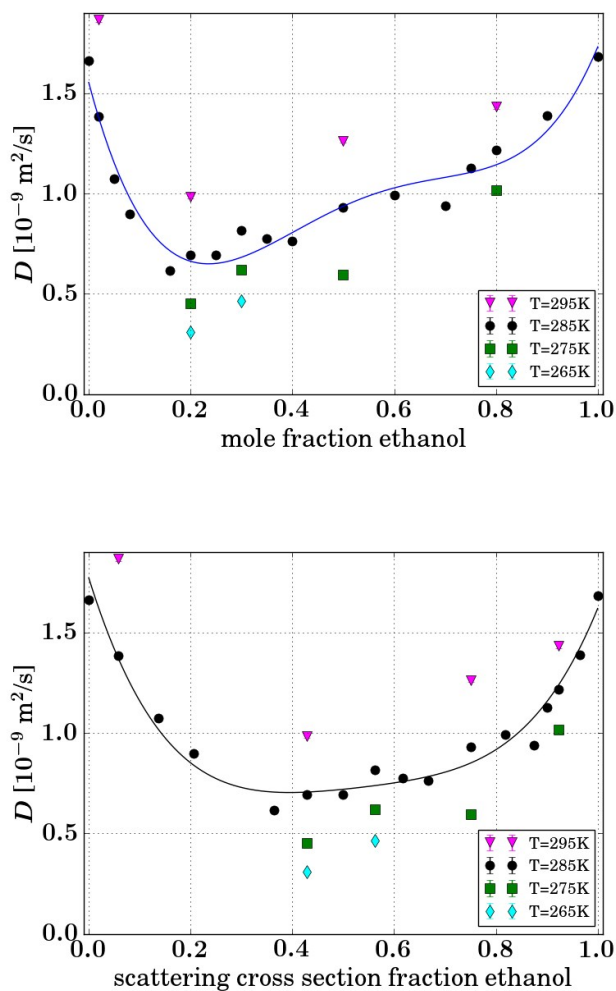
$$\sigma_1(q) = \frac{Dq^2}{1 + Dq^2 \tau}, \quad (2)$$

was imposed to describe the q-dependence of the first (narrower) Lorentzian. Therein, D is the jump-diffusion coefficient and τ the residence time.
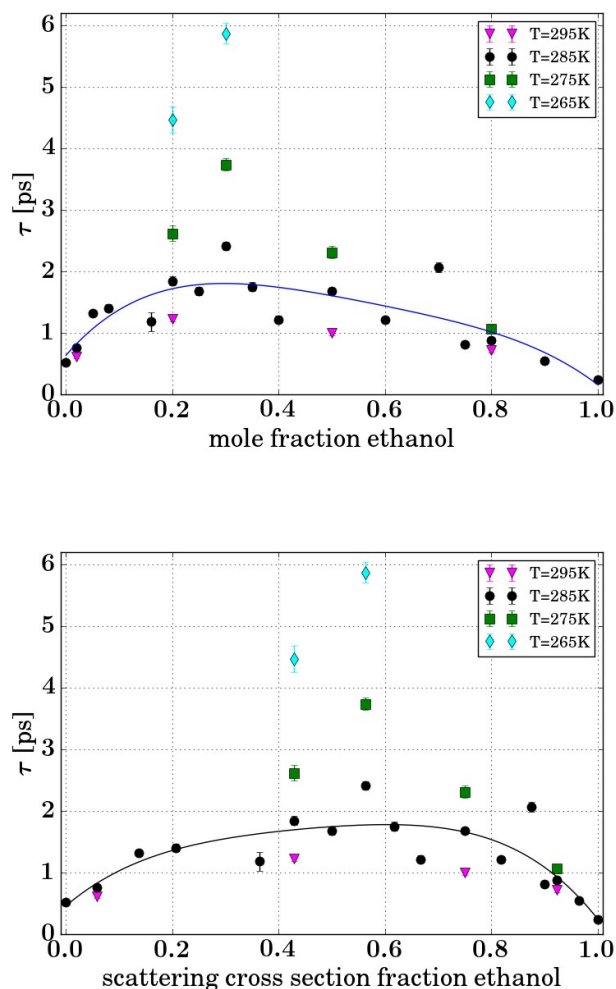
This approach resulted in stable fits for all water-ethanol ratios, whilst when leaving the q-dependence of σ_1 free, unstable fits occurred for some intermediate water-ethanol mixtures. The fit range for these global fits was 0.55 Å$^{-1} \leq q \leq 2.05$ Å^{-1}. We note that at the elevated temperatures of our samples, we did not separate the rotational and translational contributions to the diffusion, as this separation would only reliably be possible at low temperatures in the supercooled state of water.[34] For this reason, the obtained apparent diffusion coefficient $D = (1.674 \pm 0.031) \, 10^{-9}$ m^2/s for pure water

Fig. 1 Example spectra (symbols) recorded on LET (ISIS, U.K.) on a water-ethanol mixture at 0.4 mole fraction ethanol and $T = 285\,$K for two values of the scattering vector: $q = 1.25\,\text{Å}^{-1}$ (top) and $q = 1.75\,\text{Å}^{-1}$ (bottom) using the incident neutron energy 3.4 meV. The thick solid lines superimposed on the spectra denote fits by equation 1 convoluted with the spectrometer resolution. The thin solid and dashed lines report the two Lorentzian components assumed in the model. The dotted lines represent the spectrometer resolution function.

Fig. 2 Diffusion coefficients D (symbols) fitted to the spectra recorded using the incident neutron energy 3.4 meV in a global fit for all q at once of equation 2 inserted in equation 1, as a function of the water-ethanol ratio, for different temperatures. D describes the averaged self-diffusion of the water and ethanol molecules. The lines denote spline fits to the diffusion coefficients at $T = 285\,$K, as guides to the eye. The upper plot displays the results versus the mole fraction of ethanol of the samples as prepared. The lower plot displays the same results versus the calculated scattering cross section fraction of ethanol in the samples.
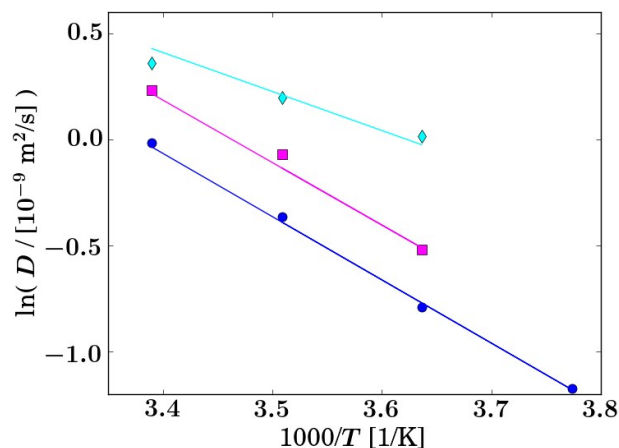
Fig. 3 Residence times τ (symbols) fitted to the spectra recorded using the incident neutron energy 3.4 meV in a global fit for all q at once of equation 2 inserted in equation 1, as a function of the water-ethanol ratio, for different temperatures. τ describes the averaged residence time of the water and ethanol molecules. The lines denote spline fits to the residence times at $T = 285$ K, as guides to the eye. The upper plot displays the results versus the mole fraction of ethanol of the samples as prepared. The lower plot displays the same results versus the calculated scattering cross section fraction of ethanol in the samples.

(H_2O) at $T = 285$ K from our experiments is slightly larger than the corresponding value obtained by gradient spin-echo NMR, $D_{NMR} = (1.58 \pm 0.08) \, 10^{-9} \, m^2/s$,[35] which is sensitive to the translational part of the self-diffusion only.

σ_2 in equation 1 can be attributed to faster motions at the limit of the accessible energy window.[32] Attempts to further extend the model to account for the different populations, namely water and ethanol, separately, led to inconclusive results and insufficient fits. Notably, in addition to independent water and ethanol contributions, a model of coupled contributions based on a generalized jump-diffusion model of multiple diffusive states was also tested.[36] This model of coupled contributions did not result in stable fits, presumably due to very similar linewidths of the two diffusive contributions attributed to the water and ethanol molecules, respectively. This behaviour is consistent with the similar absolute values of self-diffusion for the two molecules found in simulations accessing long observation times and indistinguishable contributions in the limit of short observation times (see further below for a detailed discussion).[25,37] Therefore, the single linewidth σ_1 accounts for the combined contributions from the different solvent molecules water and ethanol. Following ref.[32], the broader linewidth $\sigma_2 \gg \sigma_1$ accounts for an apparent background due to vibrational contributions and will not be further treated in this article. Nevertheless, the resulting fit parameters for this contribution are reported in the ESI (figure S4). Moreover, the Elastic Incoherent Structure Factor (EISF) $A_0(q) = a_1(q)/(a_1(q) + a_2(q))$ associated with the ratio of the two Lorentzian intensities in equation 1 agrees well with the published result for pure water[32] (figure S5) and changes with rising ethanol fraction, indicating that the confinement geometry of the diffusive motions does change by the addition of ethanol.

Example spectra along with fits are depicted in figure 1 and in figures S2 and S3 in the ESI. The diffusion coefficients D and residence times τ obtained by fitting the jump diffusion model equation 2 inserted in equation 1 are summarized in figures 2 and 3, respectively, and numerical values are listed in table S1 in the ESI. In figures 2 and 3, the x-axis denotes the mole fraction of ethanol in the samples as prepared, and the scattering cross section fraction of ethanol has been calculated from this mole fraction by the ratio of the number density of hydrogen atoms on ethanol over the total hydrogen number density. The error bars in figures 2 and 3 mark the 68% confidence limits from the diagonal of the covariance matrix and are quite small due to the global fit of the spectra for all q-values at once, imposing the jump-diffusion model, equation 2. The diffusion coefficients D (figure 2) evidence a minimum at an intermediate ethanol mole fraction, consistent with simulations,[25] and the associated residence times τ (figure 3) display a corresponding maximum very close to the ethanol mole fraction with a minimum of D.

Fig. 4 Arrhenius plot of the diffusion coefficients D (figure 2) summarized for 0.2 (circles), 0.5 (squares), and 0.8 (diamonds) mole fraction ethanol, respectively. The lines denote linear fits of $\ln(D \times 10^9 \mathrm{s/m^2}) = c_1 + c_2 \times 1000\mathrm{K}/T$. (cf. text for details)

The obtained self-diffusion coefficients can be summarized in an Arrhenius plot as illustrated in figure 4 for the 0.2, 0.5, and 0.8 ethanol mole fractions measured at different temperatures, from which Arrhenius activation energies and Arrhenius rate constants can be obtained by linear fits $\ln(D \times 10^9 \mathrm{s/m^2}) = c_1 + c_2 \times 1000\mathrm{K}/T$, where $c_{1,2}$ are scalar fit parameters.[38] For our data, the slope c_2 results in the Arrhenius activation energy E_a, defined as $D(T) = A \exp(-E_a/(k_B T))$, of $E_a = (24.79 \pm 0.25)\,\mathrm{kJ/mol}$ for the 0.2 ethanol mole fraction (figure 4).[38] Using data for the other two ethanol mole fractions, the Arrhenius activation energy E_a shows with 24.48 ± 0.98 (0.5 mol ethanol) and 10.95 ± 0.37 kJ/mol (0.8 mol ethanol) a reasonably good correlation with calculated values.[37] According to these literature values[37], the activation energy spikes around the ethanol mole fraction of 0.2, for which the lowest diffusion coefficients have been determined. The pre-exponential factor A extracted from the same fits of the Arrhenius behaviour (figure 4) gives the rate constant associated with the diffusion. The values resulting from our fits are $c_1 = \ln(A/(10^{-9}\mathrm{m^2/s})) = (10.07 \pm 0.32)$, (10.20 ± 1.22), and (4.82 ± 0.45) for the 0.2, 0.5, and 0.8 mole fraction ethanol samples, respectively. We note that the Arrhenius fits for the data with only three different temperatures are rather unstable, and further data at additional temperatures with a wider spacing would be required.

On the short picosecond observation time scales, the water and ethanol diffusion coefficients are expected to be indistinguishable according to recent simulations accessing this scale.[37] This expectation is reasonable, because on this observation time, the diffusive displacement $\sqrt{\langle r^2 \rangle}$ with $\langle r^2 \rangle = 6Dt$

is on the order of a few Ångströms, i.e. on the order of the size of the molecules. Furthermore, even on much longer time scales, such as those accessed by NMR techniques, the water and ethanol diffusion coefficients are rather similar according to earlier simulations.[25]

Moreover, in the limiting cases of 0 and 1 ethanol mole fraction only one molecular species, i.e. water or ethanol, contributes to the measured signal. It is therefore not possible to access any differences in the diffusivities of the two species in these limiting cases experimentally, but only by simulations. The absolute values of the self-diffusion coefficients found in our study on the picosecond time scale and nanometer length scale tend to be somewhat larger than the values found on much longer time and length scales using experimental NMR spectroscopy data,[27] as well as corresponding long-time simulations.[25] This observation can be understood by the larger initial slope of the diffusive mean-squared displacement versus time found in simulations on the picosecond time scale.[37]

Finally, our finding of the absence of different individual diffusivities of water and ethanol on the picosecond observation time scale does not contradict the picture of a microstructure of water and ethanol, as it has been reported that clusters resulting from such micro-structuring are short-lived with an expected lifetime of less than a picosecond, i.e. on the order of or less than the residence time τ found in our fits.[18,39] Therefore, in this respect the water-ethanol system is substantially different from other binary liquid system, e.g. dimethylsulfoxide-water mixtures, which has been studied earlier using neutron spectroscopy and which displays much longer cluster lifetimes on the order of several tens of picoseconds.[39,40]

As outlined earlier, our study on fully protiated samples may in the future be complemented by a study of water-ethanol mixtures using partially deuterated molecules combined with neutron polarization analysis in order to distinguish the contributions from the molecular constituents of the mixtures. The data presented here will support a meaningful discussion on the influence of altered mass due to the deuteration, allowing for further elucidation of this surprisingly complicated mixed-solvent system.

4 Conclusions

We have presented systematic data of the ensemble-averaged self-diffusion coefficients of water and ethanol as a function of the water-ethanol mixing ratio measured on the picosecond time scale and nanometer length scale using incoherent quasi-elastic neutron scattering. The observation time scale is crucial to interpret the results. With this understanding, our results fit in an overall picture with published simulations and experimental data using NMR spectroscopy, in which the dif-

fusivities attributed to the water and ethanol molecules, respectively, are comparable on the picosecond observation time scale that we probe with our experiment. Small differences would be expected to become apparent only on much longer time scales. The very good quality of the fits suggests that the used model, originally established for pure water, also holds for all water-ethanol mixing ratios in a sufficient approximation for the present data.

Data accessibility

The neutron data are permanently stored by the ISIS Neutron and Muon Facility and can be accessed by the experiment number RB1610311, DOI: 10.5286/ISIS.E.73947887.

Acknowledgement

References

1 J. Sellman, G. Robinson and R. Beasley, *Journal of Psychopharmacology*, 2009, **23**, 94–100.

2 J. Altman, B. Everitt, T. Robbins, S. Glautier, A. Markou, D. Nutt, R. Oretti and G. Phillips, *Psychopharmacology*, 1996, **125**, 285–345.

3 K. Gilani, A. R. Najafabadi, M. Barghi and M. Rafiee-Tehrani, *Journal of Pharmaceutical Sciences*, 2005, **94**, 1048–1059.

4 M. Malmsten, *Soft Matter*, 2006, **2**, 760–769.

5 C. Capello, U. Fischer and K. Hungerbühler, *Green Chemistry*, 2007, **9**, 927–934.

6 A. E. Farrell, R. J. Plevin, B. T. Turner, A. D. Jones, M. O'hare and D. M. Kammen, *Science*, 2006, **311**, 506–508.

7 N. J. Russell and G. W. Gould, *Food preservatives*, Springer Science & Business Media, 2003.

8 B. González, N. Calvar, E. Gómez and A. Domínguez, *The Journal Chemical Thermodynamics*, 2007, **39**, 1578 – 1588.

9 J. V. Herráez and R. Belda, *Journal of Solution Chemistry*, 2006, **35**, 1315–1328.

10 R. Belda, J. V. Herráez and O. Diez, *Physics and Chemistry of Liquids*, 2004, **42**, 467–479.

11 I. Lee, K. Park and J. Lee, *Sensors and Actuators A: Physical*, 2013, **194**, 62–66.

12 A. Nose and M. Hojo, *Journal of Bioscience and Bioengineering*, 2006, **102**, 269–280.

13 F. Franks and D. J. G. Ives, *Quarternal Reviews of the Chemical Society*, 1966, **20**, 1–44.

14 P. Sillrén, A. Matic, M. Karlsson, M. Koza, M. Maccarini, P. Fouquet, M. Götz, T. Bauer, R. Gulich, P. Lunkenheimer *et al.*, *The Journal of Chemical physics*, 2014, **140**, 124501.

15 C. Bertrand, J. Self, J. Copley and A. Faraone, *The Journal of Chemical Physics*, 2017, **146**, 194501.

16 J. Cardona, M. B. Sweatman and L. Lue, *The Journal of Physical Chemistry B*, 2018, **122**, 1505 – 1515.

17 J. Turner and A. Soper, *The Journal of Chemical physics*, 1994, **101**, 6116–6125.

18 A. Wakisaka and K. Matsuura, *Journal of Molecular Liquids*, 2006, **129**, 25–32.

19 J. F. Brandts and L. Hunt, *Journal of the American Chemical Society*, 1967, **89**, 4826–4838.

20 M. A. Amin, R. Halder, C. Ghosh, B. Jana and K. Bhattacharyya, *The Journal of Chemical Physics*, 2016, **145**, 235102.

21 L. Lins and R. Brasseur, *The FASEB journal*, 1995, **9**, 535–540.

22 Z. Derlacki, A. Easteal, A. Edge, L. Woolf and Z. Roksandic, *The Journal of Physical Chemistry*, 1985, **89**, 5318–5322.

23 E. J. W. Wensink, A. C. Hoffmann, P. J. van Maaren and D. van der Spoel, *The Journal of Chemical Physics*, 2003, **119**, 7308–7317.

24 L. Zhang, Q. Wang, Y.-C. Liu and L.-Z. Zhang, *The Journal of Chemical Physics*, 2006, **125**, 104502.

25 G. Guevara-Carrion, J. Vrabec and H. Hasse, *The Journal of Chemical Physics*, 2011, **134**, 074508.

26 K. R. Harris and Z. Newitt, P. J.and Derlacki, *The Journal of the Chemical Society, Faraday Trans.*, 1998, **94**, 1963–1970.

27 W. S. Price, H. Ide and Y. Arata, *The Journal of Physical Chemistry A*, 2003, **107**, 4784–4789.

28 V. Calandrini, A. Deriu, G. Onori, R. E. Lechner and J. Pieper, *The Journal of Chemical Physics*, 2004, **120**, 4759–4767.

29 T. Seydel, R. M. Edkins, C. D. Jones, J. Foster, R. Bewley, J. Aguilar and K. Edkins, *Chemical Communications*, 2018, **54**, 6340 – 6343.

30 R. Bewley, J. Taylor and S. Bennington, *Nuclear Instruments and Methods in Physics Research Section A: Accelerators, Spectrometers, Detectors and Associated Equipment*, 2011, **637**, 128 – 134.

31 O. Arnold, J.-C. Bilheux, J. Borreguero, A. Buts, S. I. Campbell, L. Chapon, M. Doucet, N. Draper, R. F. Leal, M. Gigg *et al.*, *Nuclear Instruments and Methods in Physics Research Section A: Accelerators, Spectrometers, Detectors and Associated Equipment*, 2014, **764**, 156–166.

32 J. Qvist, H. Schober and B. Halle, *The Journal of Chemical Physics*, 2011, **134**, 144508.

33 K. Singwi and A. Sjölander, *Physical Review*, 1960, **119**, 863.

34 J. Teixeira, M.-C. Bellissent-Funel, S. H. Chen and A. J. Dianoux, *Physical Reviews A*, 1985, **31**, 1913–1917.

35 K. T. Gillen, D. Douglass and M. Hoch, *The Journal of Chemical Physics*, 1972, **57**, 5117–5119.

36 F. Roosen-Runge, D. Bicout and J.-L. Barrat, *The Journal of Chemical Physics*, 2016, **144**, 204109.

37 S. Pothoczki, L. Pusztai and I. Bak, *Journal of Molecular Liquids*, 2018, **271**, 571 – 579.

38 M. Holz, S. R. Heil and A. Sacco, *Physical Chemistry Chemical Physics*, 2000, **2**, 4740–4742.

39 S. Banerjee and B. Bagchi, *The Journal of Chemical Physics*, 2013, **139**, 164301.

40 H. Bordallo, K. Herwig, B. Luther and N. Levinger, *The Journal of Chemical Physics*, 2004, **121**, 12457–12464.